Bioorganic & Medicinal Chemistry Letters 19 (2009) 1097–1100

Contents lists available at ScienceDirect

Bioorganic & Medicinal Chemistry Letters

journal homepage: www.elsevier.com/locate/bmcl

# Synthesis and SAR of potent LXR agonists containing an indole pharmacophore

David G. Washburn [a,*], Tram H. Hoang [a], Nino Campobasso [d], Angela Smallwood [d], Derek J. Parks [e], Christine L. Webb [b], Kelly A. Frank [c], Melanie Nord [c], Chaya Duraiswami [d], Christopher Evans [c], Michael Jaye [b], Scott K. Thompson [a]

[a] Department of Chemistry, Molecular Discovery Research, GlaxoSmithKline Pharmaceuticals, 709 Swedeland Road, King of Prussia, PA 19406, USA
[b] Department of Biology, Molecular Discovery Research, GlaxoSmithKline Pharmaceuticals, 709 Swedeland Road, King of Prussia, PA 19406, USA
[c] Department of Drug Metabolism and Pharmacokinetics, Molecular Discovery Research, GlaxoSmithKline Pharmaceuticals, 709 Swedeland Road, King of Prussia, PA 19406, USA
[d] Metabolic Pathways Centre for Excellence in Drug Discovery and Computational and Structural Chemistry, Molecular Discovery Research, GlaxoSmithKline Pharmaceuticals, 709 Swedeland Road, King of Prussia, PA 19406, USA
[e] Molecular Discovery Research GlaxoSmithKline, Research Triangle Park, NC 27709, USA

ARTICLE INFO

*Article history:*
Received 24 July 2008
Revised 29 December 2008
Accepted 6 January 2009
Available online 9 January 2009

*Keywords:*
LXR
Liver X receptors
Nuclear hormone receptors
Pulmonary inflammation
Diabetes
Atherosclerosis

ABSTRACT

A novel series of 1H-indol-1-yl tertiary amine LXR agonists has been designed. Compounds from this series were potent agonists with good rat pharmacokinetic parameters. In addition, the crystal structure of an LXR agonist bound to LXRα will be disclosed.



Liver X receptors (LXRα and LXRβ) are members of the type 2 family of the nuclear hormone receptors and function as transcription factors that mediate cholesterol and lipid metabolism.[1] LXRβ is ubiquitously expressed in a variety of different tissues, while LXRα is primarily expressed in the liver, adipose tissue, and macrophage.[1] These ligand-activated transcription factors form heterodimers with retinoid X receptors (RXR) and regulate the expression of a number of genes involved in reverse cholesterol transport, fatty acid and glucose metabolism.[2] In addition, LXRs inhibit lipopolysaccharide-induced macrophage expression of inflammatory mediators such as inducible nitric oxide synthase, cyclooxygenase 2 and interleukin-6 and inhibit inflammation in vivo.[3] Consequently, LXR agonists have been studied as a potential therapy for pulmonary inflammation, diabetes, and atherosclerosis.[2]

Recently, a number of structurally distinct LXR agonists have been reported. These are highlighted by 24(S),25-epoxycholesterol (**1**) and the synthetic ligand GW3965A (**2**) (Chart 1).[4–6] Compound **2**, identified from array synthesis, was described as a potent LXR αβ agonist. This compound showed good potency and full agonist activity in the LXRβ FRET ($EC_{50}$ = 25 nM) and mouse macrophage cholesterol efflux assays ($EC_{50}$ = 50 nM); however, it was less potent in the LXRα FRET assay ($EC_{50}$ = 175 nM).[4–6]

As part of an effort to identify LXR agonists with improved potency, a structure-based design strategy centering around **2** was initiated. Analysis of the X-ray crystal structure of compound **2** and other LXR agonists revealed an unoccupied hydrophobic pocket adjacent to the phenyl acetic acid region of **2**.[6,7] Toward this end, we set out to explore suitable replacements for the phenyl acetic acid moiety of **2**.

Synthesis of the analogs of **2** is outlined in Scheme 1. Reductive amination of benzaldehyde **4** with 2,2-diphenylethanamine **3** yielded the secondary amine **5**. Subsequent treatment of **5** with base and 3-bromo-1-propanol or 1,3-dibromopropane yielded the desired alcohol **6** or bromide **7**, respectively. Intermediates **6** and **7** served as important building blocks for exploration of replacements for the phenyl acetic acid group. Target heteroaromatic ethers **8–15** were then prepared by either Mitsunobu coupling of **6** or nucleophilic displacement of alkyl bromide **7**.

Analogs **8–15** all displayed potencies in the LXRαβ FRET assay comparable to the lead **2** (Table 1); however, only **15** displayed full agonism (>80% compared to the reference agonist **2**). In addition, compound **15** showed improved potency in the mouse macrophage cholesterol efflux assay compared to **2**. Due to these results, we focused our attention on modifying compound **15**.

* Corresponding author. Tel.: +1 610 270 4941.
*E-mail address:* dave.g.washburn@gsk.com (D.G. Washburn).

0960-894X/$ - see front matter © 2009 Elsevier Ltd. All rights reserved.
doi:10.1016/j.bmcl.2009.01.004

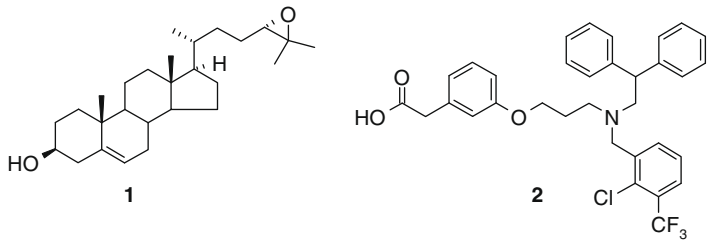


**Chart 1.** Structures of 24(S),25-epoxycholesterol (**1**) and GW3965A (**2**).

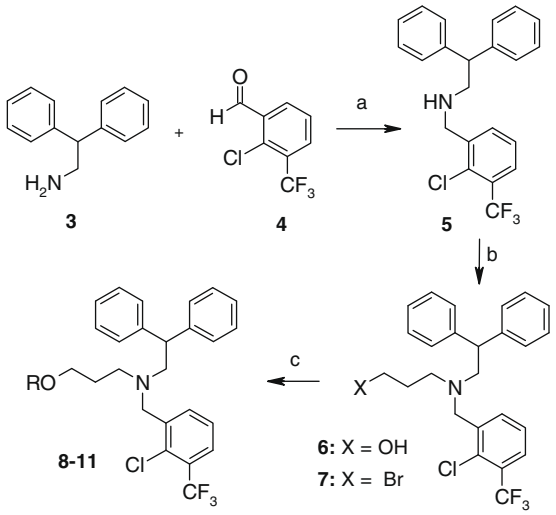


**Scheme 1.** Reagents and conditions: (a) $NaB(OAc)_3H$, (2,2-diphenylethyl)amine, AcOH, $CH_2Cl_2$,; (b) 3-bromo-1-propanol, NaI, $K_2CO_3$, $CH_3CN$ or 1,3 dibromopropane, $K_2CO_3$, $CH_3CN$; (c) ROH, DIAD, THF or ROH, $K_2CO_3$, $CH_3CN$.

A docked pose of **15** overlaid with the crystal structure of **2** bound to LXRβ suggested that while the indole was predicted to better fill the hydrophobic pockets, key hydrogen bonding to Leu330 and Arg319 were likely not be exploited as observed with **2** (Fig. 1).[7,8]

With this in mind, efforts to extend the reach of the indole nitrogen of **15** were initiated. Reaction of **15** with base and electrophiles produced compounds **16–18** (Table 1).[9] While these compounds were all equipotent to **15** in the LXRβ FRET assay, they all showed improved LXRα potency. Furthermore, while **16** and **17** displayed only partial LXRα agonist activity, **18** demonstrated full agonism against both isoforms. In addition, **18** exhibited excellent cellular activity in a mouse macrophage cholesterol efflux assay (Scheme 2).

The crystal structures determined for **2** (bound to LXRβ) and **18** (bound to LXRα) show clear distinctions between the two compounds (Fig. 2).[7,10] The indole ring of compound **18** but not the phenyl ring of **2** appears to fill the leucine rich hydrophobic pocket. There is also a hydrogen binding interaction (2.8 Å) between one of the carboxylate oxygens of **18** and the NH backbone of Leu314 (LXRα). In addition, there is a stronger salt bridge interaction between Arg303 (LXRα) and one of the carboxylate oxygens of compound **18** with the distances being 3.1 Å and 3.2 Å while the corresponding interactions for compound **2** with Arg319 (LXRβ) are 3.6 and 3.8 Å, respectively.

Having prepared a compound with target in vitro characteristics, we next evaluated its rat pharmacokinetic properties (Table 2). In general, compound **18** displayed attractive PK properties including low clearance, small $Vd_{ss}$, moderate half-life, and good oral bioavailability.

**Table 1**
LXRαβ FRET assay data for compounds **2** and **8–18**[a]

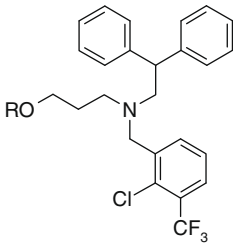


| Compound | R | LXRα $EC_{50}$, nM (% eff.) | LXRβ $EC_{50}$, nM (% eff.) | MM-Efflux $EC_{50}$, nM |
|---|---|---|---|---|
| **2** | 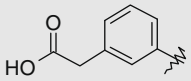 | 175 (100%) | 25 (100%) | 50 |
| **8** | 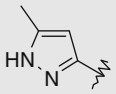 | 23 (25%) | 15 (30%) | ND |
| **9** | 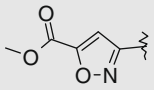 | 63 (65%) | 26 (68%) | ND |
| **10** | 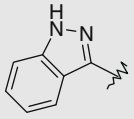 | 110 (17%) | 60 (44%) | ND |
| **11** | 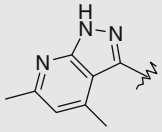 | >3000 | 510 (25%) | ND |
| **12** | 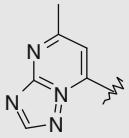 | 790 (25%) | 560 (33%) | ND |
| **13** | 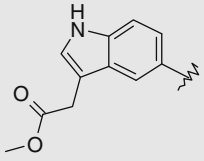 | 630 (19%) | 288 (36%) | ND |
| **14** | 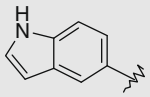 | 226 (36%) | 23 (78%) | ND |

**Table 1** (*continued*)

| Compound | R | LXRα $EC_{50}$, nM (% eff.) | LXRβ $EC_{50}$, nM (% eff.) | MM-Efflux $EC_{50}$, nM |
|---|---|---|---|---|
| **15** | 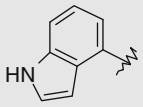 | 60 (90%) | 15 (104%) | 5.0 |
| **16** | 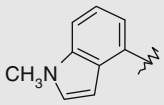 | 39 (57%) | 12 (86%) | ND |
| **17** | 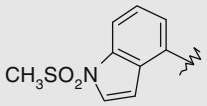 | 20 (50%) | 7 (72%) | ND |
| **18** | 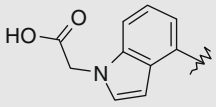 | 14 (132%) | 4 (105%) | 15 |

$EC_{50}$ = concentration of compound that leads to half-maximal activity.
% efficacy (eff. = efficacy) normalized to **2**. ND = no data available.

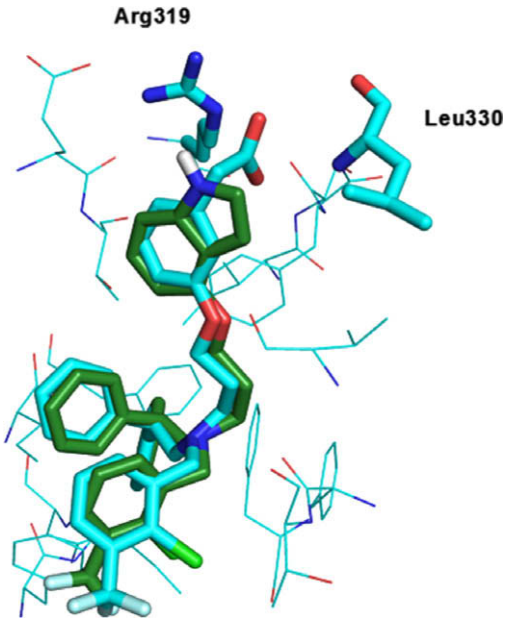


**Figure 1.** Overlay of the crystal structure of **2** (cyan) bound to the LBD of LXRβ and **15** (green).

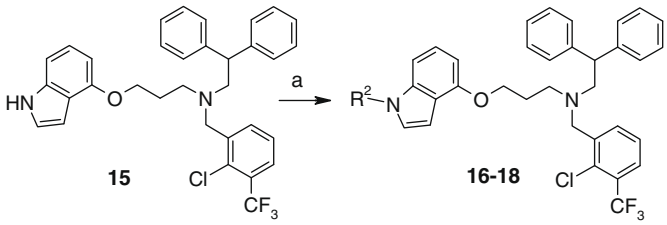


**Scheme 2.** (a) NaH, electrophile, DMF.

In summary, replacement of the phenyl acetic acid head group of the lead compound **2** with 1H-indol-1-yl acetic acid group led to a novel orally bioavailable LXR agonist **18**. Compared to **2**, **18** showed much improved potency and efficacy in the LXRα FRET, and potencies in the LXRβ FRET and in mouse macrophage cholesterol efflux assays were also improved. In addition, this indole-based LXR agonist described has properties suitable for in vivo testing, the results of which are to be described in a further publication.

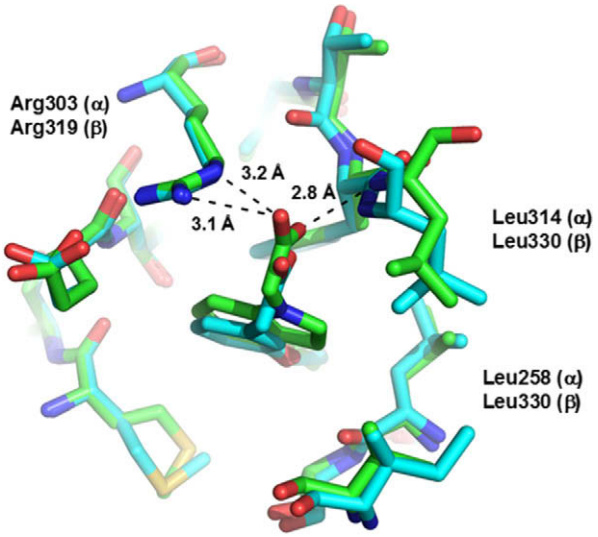


**Figure 2.** Superposition of crystal structures of **18** (green) bound to the LXRα-LBD & **2** (cyan) bound to the LXRβ-LBD. Enzyme backbone and key backbone residues are shown in the color of the ligand to which they correspond.

**Table 2**
In vivo rat pharmacokinetic data for compound **18**[a,b]

| Parameter | Compound **18**[a] |
|---|---|
| Dose (iv, p.o., mg/kg) | 1.1, 2.1 |
| CLp (mL/min/kg) | 14.6 (1.7) |
| $Vd_{ss}$ (L/kg) | 1.15 (0.29) |
| $t_{½}$, i.v. (h) | 1.35 (.5) |
| Oral Cmax (ng/mL) | 1808 (134) |
| $t_{½}$, p.o. (h) | 2.9 (1.2) |
| Oral%F | 45.4 (5.8) |

[a] Values are means of three experiments, standard deviation is given in parentheses.
[b] Male Sprague–Dawley rats (<1 year old) were used.

## References and notes

1. (a) Jaye, M. *Curr. Opin. Investig. Drugs* **2003**, *4*, 1053; (b) Collins, J. L. *Curr. Opin. Drug Discov. Dev.* **2004**, *7*, 692; (c) Lund, E. G.; Menke, J. G.; Sparrow, C. P. *Arterioscl. Throm. Vas.* **2003**, *237*, 1169.
2. (a) Repa, J. J.; Turley, S. D.; Lobaccaro, J.-M. A.; Medina, J.; Li, L.; Lustig, K.; Shan, B.; Heyman, R. A.; Dietschy, J. M.; Mangelsdorf, D. J. *Science* **2000**, *289*, 1524; (b) Levin, N.; Bischoff, E. D.; Daige, C. L.; Thomas, D.; Vu, C. T.; Heyman, R. A.; Tangirala, R. K.; Schulman, I. G. *Arterioscl. Throm. Vasc.* **2005**, *25*, 135; (c) Laffitte, B. A.; Chao, L. C.; Li, J.; Walczak, R.; Hummasti, S.; Joseph, S. B.; Castrillo, A.; Wilpitz, D. C.; Mangelsdorf, D. J.; Collins, J. L.; Saez, E.; Tontonoz, P. *Proc. Natl. Acad. Sci. U.S.A.* **2003**, *100*, 5419; (d) Chisholm, J. W.; Hong, J.; Mills, S. A.; Lawn, R. M. *J. Lipid Res.* **2003**, *44*, 2039; (e) Smoak, K.; Madenspacher, J.; Jeyaseelan, S.; Williams, B.; Dixon, D.; Poch, K. R.; Nick, J. A.; Worthen, G. S.; Fessler, M. B. *J. Immunol.* **2008**, *180*, 3305.
3. Joseph, S. B.; Castrillo, A.; Laffitte, B. A.; Mangelsdorf, D. J.; Tontonoz, P. *Nat. Med.* **2003**, *9*, 213.
4. (a) Lehmann, J. M.; Kliewer, S. A.; Moore, L. B.; Smith-Oliver, T. A.; Blanchard, D. E.; Spencer, T. A.; Willson, T. M. *J. Biol. Chem.* **1997**, *272*, 3137; (b) Meinke, P. T.; Wood, H. B.; Szewczyk, J. W. *Annu. Rep. Med. Chem.* **2006**, *41*, 99.
5. Collins, J. L.; Fivush, A. M.; Watson, M. A.; Galardi, C. M.; Lewis, M. C.; Moore, L. B.; Parks, D. J.; Wilson, J. G.; Tippin, T. K.; Binz, J. G.; Plunket, K. D.; Morgan, D. G.; Beaudet, E. J.; Whitney, K. D.; Kliewer, S. A.; Willson, T. M. *J. Med. Chem.* **2002**, *45*, 1963.

6. (a) Jaye, M. C.; Krawiec, J. A.; Campobasso, N.; Smallwood, A.; Qiu, C.; Lu, Q.; Kerrigan, J. J.; De Los Frailes Alvaro, M.; Laffitte, B.; Liu, W.; Marino, J. P., Jr.; Meyer, C. R.; Nichols, J. A.; Parks, D. J.; Perez, P.; Sarov-Blat, L.; Seepersaud, S. D.; Steplewski, K. M.; Thompson, S. K.; Wang, P.; Watson, M. A.; Webb, C. L.; Haigh, D.; Caravella, J. A.; Macphee, C. H.; Wilson, T. M.; Collins, J. L. *J. Med. Chem.* **2005**, *48*, 5419; (b) Schultz, J. R.; Tu, H.; Luk, A.; Repa, J. J.; Medina, J. C.; Li, L.; Schwendner, S.; Wang, S.; Thoolen, M.; Mangelsdorf, D. J.; Lustig, K. D.; Shan, B. *Gene Dev.* **2000**, *14*, 2831. Role of LXRs in control of lipogenesis.
7. (a) Faernegardh, M.; Bonn, T.; Sun, S.; Ljunggren, J.; Ahola, H.; Wilhelmsson, A.; Gustafsson, J.-A.; Carlquist, M. *J. Biol. Chem.* **2003**, *278*, 38821; (b) Svensson, S.; Oestberg, T.; Jacobsson, M.; Norstroem, C.; Stefansson, K.; Hallen, D.; Johansson, I. C.; Zachrisson, K.; Ogg, D.; Jendeberg, L. *EMBO J.* **2003**, *22*, 4625; (c) Williams, S.; Bledsoe, R. K.; Collins, J. L.; Boggs, S.; Lambert, M. H.; Miller, A. B.; Moore, J.; McKee, D. D.; Moore, L.; Nichols, J.; Parks, D.; Watson, M.; Wisely, B.; Willson, T. M. *J. Biol. Chem.* **2003**, *278*, 27138; (d) Hoerer, S.; Schmid, A.; Heckel, A.; Budzinski, R.-M.; Nar, H. *J. Mol. Biol.* **2003**, *334*, 853.
8. Compound **15** was docked using the program, Flo+, version 0203 as shown in McMartin, C.; Bohacek, R. S. *J. Comput.-Aided Mol. Des.* **1997**, *11*, 333–334. The protein coordinates containing polar hydrogen were converted to Macromodel format using Flo+ tools. All residues within a 20 Å sphere centered on a residue identified visually as central in the binding site were selected, and the rest of the protein atoms were removed. The residues lining the binding site pocket (approximately 10 Å from same residue near the center of the active site) were selected to allow movement during minimization steps. The remaining residues were held rigid during all docking and minimization calculations. The *mcdock* algorithm, which relies on a Monte Carlo perturbation/fast search/energy minimization algorithm was used for this study. Two thousand steps of perturbation were performed and the twenty-five top-ranked poses were retained. Visual inspection of the interactions made by the ligand within the active site and the relative strain energies of the protein and ligand in each pose was used to determine the best docked pose. The figures were made using the Pymol software. DeLano, W.L. The PyMOL Molecular Graphics System (2002) DeLano Scientific, San Carlos, CA, USA on the World Wide Web; http://www.pymol.org.
9. Example preparation: Compound **18**. Step 1: To a solution of 2,2-diphenethylamine (2.0 g, 10.0 mmole) and 2-chloro-3-trifluoromethylbenzaldehyde (2.33 g, 11.0 mmole) in $CH_2Cl_2$ (20 mL) was added $NaB(OAc)_3H$ (2.36 g, 11.0 mmole) and AcOH (2.0 mL). After the reaction mixture stirred overnight, solvent was removed and the residue was washed with saturated $NaHCO_3$, and extracted with EtOAc (3×). The organic extracts were dried over $Na_2SO_4$, filtered, and concentrated. Purification via silica gel column chromatography (silica gel 60, EM Science) afforded the product (3.0 g, 76% yield). $^1H$ NMR ($CDCl_3$): δ 7.62 (d, $J$ = 8 Hz, 1H), 7.58 (d, $J$ = 7.2 Hz, 1H), 7.35–7.22 (m, 11H), 4.26 (t, $J$ = 7.6 Hz, 1H), 4.00 (s, 2H), 3.28 (d, $J$ = 7.6 Hz, 2H). MS(ES) $m/e$ 390.0 $[M+H]^+$. Step 2: $K_2CO_3$ (0.53 g, 3.85 mmol) was added to a solution of [2-chloro-3-trifluoromethyl-benzyl](2,2-diphenylethyl)amine (1.00 g, 2.56 mmol), dibromopropane (2.60 mL, 25.6 mmol) and $CH_3CN$ (25.6 mL). After the reaction mixture was refluxed overnight, it was poured into saturated $NH_4Cl$ and extracted with EtOAc (3×). The organic layers were combined, dried over $Na_2SO_4$, filtered, and concentrated. Purification via silica gel chromatography yielded the product (1.10 g, 84%). $^1H$ NMR ($CDCl_3$): $\delta$ 7.57 (d, $J$ = 7.6 Hz, 1H), 7.33–7.14 (m, 12H), 4.18 (t, $J$ = 7.6 Hz, 1H), 3.79 (s, 2H), 3.24 (t, $J$ = 6.4 Hz, 2H), 3.15 (d, $J$ = 7.6 Hz, 2H), 2.72 (t, $J$ = 6.4 Hz, 2H), 1.95 (m, 2H) MS(ES) $m/e$ 510.2 $[M+H]^+$. MS(ES) $m/e$ 510.2 $[M+H]^+$. Step 3: To a sealed tube (3-bromo-propyl)-(2-chloro-3-trifluoromethyl-benzyl)-2,2-diphenyl-ethyl-amine (250 mg, 0.49 mmol), 4-hydroxyindole (79 mg, 0.50 mmol), $K_2CO_3$ (388 mg, 2.50 mmol), and $CH_3CN$ (3 mL) were added and heated at 90 °C overnight. The mixture was filtered, concentrated, and purified via silica gel chromatography to yield the product (270 mg, 98%). $^1H$ NMR ($CDCl_3$): $\delta$ 8.14 (s, 1H), 7.45 (d, $J$ = 7.6 Hz, 1H), 7.30–7.05 (m, 14H), 6.87 (m, 1H), 6.61 (m, 1H), 6.44 (d, $J$ = 7.6 Hz, 1H), 4.22 (m, 1H), 3.99 (t, $J$ = 6 Hz, 2H), 3.86 (s, 2H), 3.21 (d, $J$ = 7.6 Hz, 2H), 2.87 (t, $J$ = 6 Hz, 2H), 2.01 (m, 2H). MS(ES) $m/e$ 563.0 $[M+H]^+$. Step 4: To a solution of NaH (60% in oil) (6.79 g, 172.2 mmol) and DMF (100 mL), a mixture of (2-chloro-3-trifluoromethyl-benzyl)-(2,2-diphenyl-ethyl)-[3-(1*H*-indol-4-yloxy)-2-methyl-propyl]-amine (9.70 g, 17.2 mmol) and DMF (100 mL) was added. After the mixture stirred 0.25 h, $BrCH_2COOH$ (12.0 g, 84.9 mmol) was added and the mixture was stirred overnight. The reaction mixture was then poured into 1 N HCl and extracted with EtOAc. The organic layers were combined, dried over $Na_2SO_4$, filtered, and concentrated. Purification via preparative HPLC yielded the product which was dissolved in $Et_2O$, acidified with 1 N HCl in $Et_2O$, and concentrated to afford the desired product as the HCl salt (7.16 g, 67%). mp 197–199 °C; $^1H$ NMR ($CDCl_3$): $\delta$ 7.97 (b, s, 1H), 7.60 (d, $J$ = 8 Hz, 1H), 7.26–7.20 (m, 11H), 6.99 (m, 2H), 6.85 (d, $J$ = 2.4 Hz, 1H), 6.58 (dd, $J$ = 8.8 Hz, 2 Hz, 1H), 6.42 (d, $J$ = 3.2 Hz, 1H), 4.78 (s, 2H), 4.49 (m, 1H), 4.12 (s, 2H), 3.65 (m, 2H), 3.56 (m, 2H), 2.99 (m, 2H), 1.90 (m, 2H). MS(ES) $m/e$ 621.2 $[M+H]^+$.
10. Protein was expressed, purified and crystallized as in Ref. 6. The X-ray diffraction data were collected at sector 17ID at the Advanced Photon Source, Argonne National Laboratory. The X-ray diffraction images were processed with HKL2000 (Otwinowski, Z. and Minor, W. *Methods Enzymol.* **1997**, *276*, 307–326). The protein crystallized in the space group C2 with cell dimensions $a$ = 122.2 Å, $b$ = 90.0 Å, $c$ = 101.6 Å, and $b$ = 111.9 degr and with two heterodimers per asymmetric unit. The Rmerge and completeness of the data to 2.06 Å resolution were 8.2% and 93%, respectively. The structure was solved by molecular replacement using PHASER (McCoy, A. J., Grosse-Kunstleve, R. W.; Adams, P. D.; Winn, M. D.; Storoni, L.C.; Read, R. J. *J. Appl. Cryst.* **2007**, *40*, 658–674.) and using starting coordinates from PDB id = 2ACL. The model was built and refined with COOT (Emsley, P. & Cowtan, K. *Acta. Cryst. D.* **2004**, *60* 2126–2132) and PHENIX.REFINE (Afonine, P. V.; Grosse-Kunstleve, R. W. & Adams; P. D. **2005**. CCP4 Newsl. 42, contribution 8). The model was refined to an R factor of 20% and R free of 25%. Protein coordinates were deposited: RCSB ID code rcsb050408 and PDB ID code 3FC6.